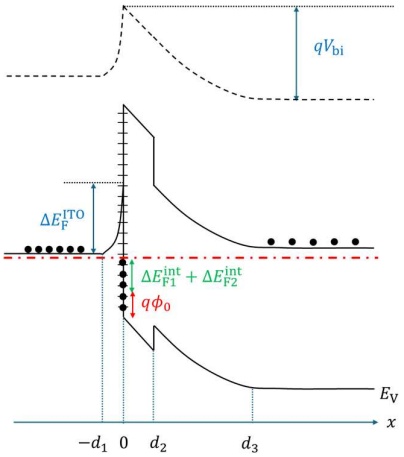

Fig. 1. Band diagram at equilibrium after the charge transfer. The diagram shows a back-to-back N+-p-n junction (N+: heavily doped wide bandgap materials), while the N+-p junction behaves as a tunnel junction due to high electron concentration in the ITO layer.

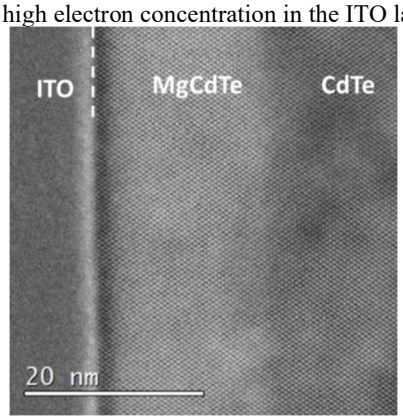

Fig. 3. Atomic-resolution cross-sectional STEM image revealing excellent crystallinity and sharply defined interfaces between the ITO, MgCdTe, and CdTe layers. Each layer is clearly labeled, and the interface between the ITO and the MgCdTe barrier is indicated by a dashed line.

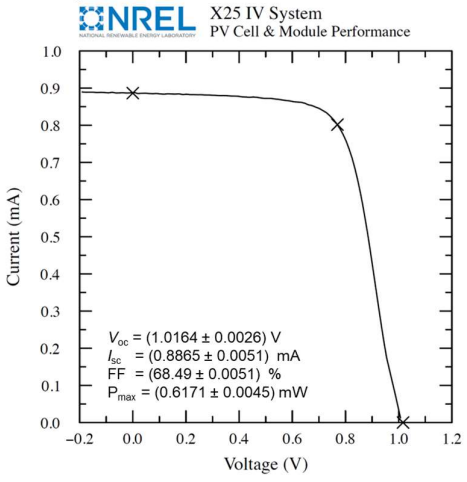

Fig. 5. NREL certified device results. *I-V* curve of the best solar cell device with AR coating.

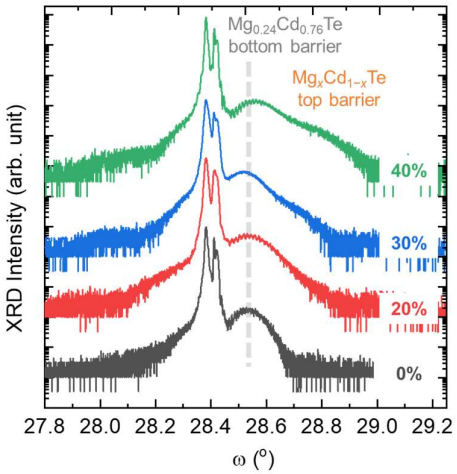

Fig. 2. Coupled ω-2θ scans of the (004) reflection for the CdTe/MgCdTe DH layers grown on InSb (001) substrates.

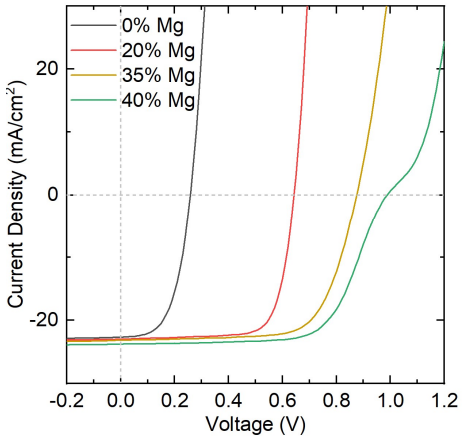

Fig. 4. J-V curves of solar cell devices with different Mg compositions in the top barrier layers under one-sun illumination.

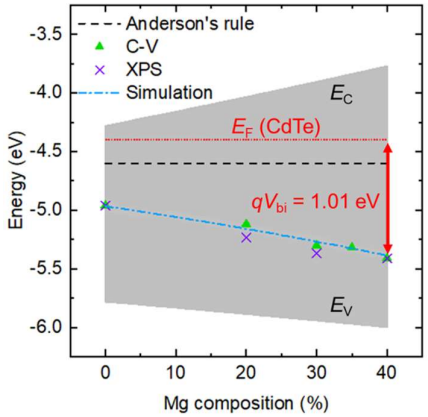

Fig. 6. The summary of ITO/MgCdTe interface Fermi-level positions determined through Anderson's model, *C-V*, and XPS measurements are indicated for comparison